Preoperative computed tomography-guided disease-free survival prediction in gastric cancer: a multicenter radiomics study

Authors： Siwen Wang[1,2#], Caizhen Feng[3#], Di Dong[1,2#], Hailin Li[1,2], Jing Zhou[4], Yingjiang Ye[4], Zaiyi Liu[5*], Jie Tian[1,6*], Yi Wang[3*]

Affiliations:

[1] CAS Key Laboratory of Molecular Imaging, Institute of Automation, Chinese Academy of Sciences, Beijing, 100190, China

[2] School of Artificial Intelligence, University of Chinese Academy of Sciences, Beijing, 100049, China

[3] Department of Radiology, Peking University People's Hospital, Beijing, 100044, China

[4] Department of Gastrointestinal Surgery, Peking University People's Hospital, Beijing, 100044, China

[5] Department of Radiology, Guangdong Provincial People's Hospital, Guangdong Academy of Medical Sciences, Guangzhou, 510080, China

[6] Beijing Advanced Innovation Center for Big Data-Based Precision Medicine, Beihang University, Beijing, 100191, China

Siwen Wang[#], Caizhen Feng[#], and Di Dong[#] should be considered joint first authors.

***Corresponding authors:**

Yi Wang, MD

Department of Radiology, Peking University People's Hospital, Beijing, 100044, China

Email: wangyi@pkuph.edu.cn

Jie Tian, PhD

Fellow of ISMRM, IEEE, AIMBE, IAMBE, IAPR, SPIE, OSA

CAS Key Laboratory of Molecular Imaging, Institute of Automation, Chinese Academy of Sciences, Beijing, 100190, China

Email: jie.tian@ia.ac.cn

Zaiyi Liu, MD

This article has been accepted for publication and undergone full peer review but has not been through the copyediting, typesetting, pagination and proofreading process, which may lead to differences between this version and the Version of Record. Please cite this article as doi: 10.1002/MP.14350

Department of Radiology, Guangdong Provincial People's Hospital, Guangdong Academy of Medical Sciences, Guangzhou, 510080, China

Email: zyliu@163.com

Preoperative computed tomography-guided disease-free survival prediction in gastric cancer: a multicenter radiomics study

Abstract

Purpose: Preoperative and noninvasive prognosis evaluation remains challenging for gastric cancer. Novel preoperative prognostic biomarkers should be investigated. This study aimed to develop multidetector-row computed tomography (MDCT)-guided prognostic models to direct follow-up strategy and improve prognosis.

Methods: A retrospective dataset of 353 gastric cancer patients were enrolled from two centers and allocated to three cohorts: training cohort (n = 166), internal validation cohort (n = 83), and external validation cohort (n = 104). Quantitative radiomic features were extracted from MDCT images. The least absolute shrinkage and selection operator penalized Cox regression was adopted to construct a radiomic signature. A radiomic nomogram was established by integrating the radiomic signature and significant clinical risk factors. We also built a preoperative tumor-node-metastasis staging model for comparison. All models were evaluated considering abilities of risk stratification, discrimination, calibration, and clinical use.

Results: In the two validation cohorts, the established four-feature radiomic signature showed robust risk stratification power (P = 0.0260 and 0.0003, log-rank test). The radiomic nomogram incorporated radiomic signature, extramural vessel invasion, clinical T stage, and clinical N stage, outperforming all the other models (concordance index = 0.720 and 0.727) with good calibration and decision benefits. Also, the 2-year disease-free survival (DFS) prediction was most effective (time-dependent area under curve = 0.771 and 0.765). Moreover, subgroup analysis indicated that the radiomic signature was more sensitive in stratifying patients with advanced clinical T/N stage.

Conclusions: The proposed MDCT-guided radiomic signature was verified as a prognostic factor for gastric cancer. The radiomic nomogram was a noninvasive auxiliary model for preoperative individualized DFS prediction, holding potential in promoting treatment strategy

and clinical prognosis.

Keywords: disease-free survival, risk stratification, radiomics, gastric cancer, multidetector-row computed tomography

Introduction

Gastric cancer answers for a worldwide estimated 783,000 deaths in 2018, ranking third among leading causes of cancer death[1]. The primary treatment strategies of gastric cancer include endoscopic submucosal dissection, radical surgery, neoadjuvant therapy, and chemotherapy et al. In times of treatment decision making, clinicians and patients desperately need evidence-based information about risk of recurrence and death, which is mainly based on preoperative clinical tumor-node-metastasis (TNM) system. Nowadays, multidetector-row computed tomography (MDCT) is widely applied in clinical staging owing to its noninvasiveness, convenience, and stability[2] and clinical staging defined on preoperative MDCT has been proven a prognostic indicator of survival[3,4]. Furthermore, some other characteristics on MDCT, for instance, extramural vessel invasion, have also been proven closely related to the prognosis of gastric cancer[5,6]. However, subjective and qualitative, conventional interpretation of MDCT mainly depends on clinical experience and individual perspective of radiologists. Therefore, novel means should be investigated to accelerate individualized prognostic progress and improve outcomes for gastric cancer patients.

Recent advances of molecular markers are growing important for prognostic analysis in gastric cancer. Several studies[7,8] suggested that patients with hypermethylated MDGA2 or exhibiting imbalanced ADAR1/2 demonstrated extremely poor prognosis. Nevertheless, limited by high cost and complex protocols, most molecular markers are not yet available for application in clinical medicine.

Particularly, potential of radiomics has been revealed in recent years' studies[9-11]. The main concept lies in quantitatively mining high-throughput medical image traits and capturing tumor heterogeneity via computer-based analysis to improve diagnosis and prognosis[12,13]. In previous researches, Giganti[14] and Yoon[15] et al. evaluated the associations between CT texture features and survival outcomes. However, their studies merely used a few texture features, which might underestimate the significance of radiomics in quantifying tumor morphology and intensity on

CT images. Taking a step forward, Li[16] and Jiang[17,18] et al. established CT-based radiomic nomograms combining radiomic signatures and clinical factors to predict prognosis for gastric cancer and showed good performance, higher than models with clinical factors alone. However, the major clinical factors in above models, such as T/N stage, were determined by postoperative histopathological analysis of surgical specimens. Thus, the contribution of their models to preoperative treatment decision making is limited greatly.

Under such circumstances, this study aimed to create an MDCT-guided radiomic signature for preoperative disease-free survival (DFS) prediction in gastric cancer and verify its incremental contribution to preoperative radiomic nomogram.

Materials and Methods

Enrolled population

This multicenter retrospective study was ethically granted by the Institutional Review Board of Peking University People's Hospital (center 1) and Guangdong Provincial People's Hospital (center 2) in compliance with the Health Insurance Portability and Accountability. Informed consent was not required. In center 1, 249 pathologically confirmed gastric cancer patients (182 men and 67 women) were collected. In center 2, 104 patients (72 men and 32 women) were collected. Supplemental Text S1 and Figure S1 provided detailed inclusion and exclusion criteria along with a final diagram for patient recruitment.

Follow-up information included laboratory testing and chest/abdominal/pelvic MDCT at 3, 6, 12 months within the first year, each subsequent annual postoperatively. The progressive event was defined as local recurrent, metachronous metastatic disease, or recorded death caused by gastric cancer. DFS time was recorded in months from the radical surgery date to progressive date or the last follow-up date patients were known free of disease. Available clinical risk factors included age, sex, carcinoembryonic antigen (CEA), carbohydrate antigen 19-9 (CA19-9), location/growth pattern, clinical T stage (ctT), clinical N stage (ctN), and extramural vessel invasion (ctEMVI) defined on MDCT (Table 1). Definitions for ctT, ctN, and ctEMVI according

to Supplemental Text S2 were assessed and confirmed by three radiologists upon consistent consultation.

Patients in center 1 were randomly allocated to two cohorts at a 2:1 ratio (training cohort, n=166; internal validation cohort, n=83). Patients in center 2 were used as external validation cohort. The sample size power analysis and randomization method were given in Supplemental Text S3.

MDCT-guided feature extraction

The contrast-enhanced portal venous phase MDCT images were used in this study. Detailed procedure for image acquisition is given in Supplemental Text S4. The CT scanning parameters for the two centers are provided in Supplemental Table S1.

The tumor regions of interest (ROIs) were created by manually delineating along the tumor margin on the slice with the largest tumor area using ITK-SNAP (version 3.4.0, http://www.itksnap.org). Two-dimensional radiomic features were extracted for all the patients based on algorithms provided in Pyradiomics (version 2.1.1) and implemented by Python 3.6 (https://www.python.org). Final radiomic features were composed of eight groups according to the image biomarker standardization initiative (IBSI). Specific feature types are summarized in Supplemental Figure S2. Image quality control and feature consistency test are described in Supplemental Text S5.

Numerical radiomic features were standardized by z-score method using the mean and standard deviation parameters calculated from the training cohort. Key feature selection was conducted in the training cohort using a Cox proportional hazards regression method with the least absolute shrinkage and selection operator (LASSO) penalty in 10-fold cross-validation.

Individualized radiomic signature construction and validation

The overall radiomics workflow is depicted in Figure 1. Radiomic signature construction was conducted within the training cohort. Cox proportional hazards regression was used for modelling the radiomic signature by examining the joint effects of selected radiomic features on

the risk of disease progression at a particular survival time[19]. Reserved key radiomic features were simultaneously fed into a multivariate Cox regression to compute the regression coefficients. Then, radiomic features weighted by corresponding regression coefficients posed a linear formula to calculate an individualized risk score per patient, which was called a radiomic signature.

Potential contribution of radiomic signature to DFS was verified in the two validation cohorts. Using median radiomic signature value calculated in the training cohort as a cutoff value, patients were separated into high-risk (≥ median) and low-risk (< median) groups in each cohort. Kaplan-Meier survival curves, along with log-rank tests were conducted to investigate significant differences in risk stratification. To evaluate discrimination, concordance index (C-index) was computed. Also, the time-dependent receiver operating characteristic (ROC) curve analysis[20] was conducted to investigate how well the radiomic signature could predict the DFS at the time point of 1, 2, and 3 years. To quantify the goodness-of-fit between actual and predicted survival probabilities, calibration curves along with Hosmer-Lemeshow tests were measured. In usefulness of clinical trials, decision curve analysis (DCA) was conducted in internal validation cohort by calculating the net benefits at some threshold probabilities.

Subgroup analysis of radiomic signature according to clinical T and N stage

One remarkable trial was that we moved on to see whether radiomic signature could still well risk stratify patients with certain clinical stage. Patients from center 1 and center 2 were both divided into seven subgroups according to clinical T and N stage. The risk stratification performance was investigated using Kaplan-Meier survival curves along with log-rank tests in these subgroups, including ctT1 group, ctT2 group, ctT3 group, ctT4 group, ctN- group, ctN+ group, and neoadjuvant therapy group. Herein, recommended by National Comprehensive Cancer Network guidelines to receive neoadjuvant therapy[21], patients with ctT2 or higher ctT and any ctN constituted the neoadjuvant therapy group.

Radiomic nomogram development and performance evaluation

Clinical risk factors in Table 1 were taken into consideration to build a more powerful radiomic nomogram. Significant risk factors were screened out by both univariate and multivariate Cox regressions in the training cohort. Then the radiomic signature and selected clinical risk factors were fed into a Cox regression, giving the final potential prognostic radiomic nomogram. The outputs of the radiomic nomogram were the probabilities of DFS.

Further, a preoperative TNM staging model was established based on the training cohort using the multivariate Cox proportional hazards regression with the ctT and ctN as the covariates of estimating risk of disease progression at a particular survival time. Apart from C-index, area under the ROC curve (AUC), and DCA, comparison of the three prognostic models (radiomic signature, radiomic nomogram, TNM staging model) was quantified by integrated discrimination improvement (IDI)[22] (details in Supplemental Text S6). Thereinto, IDI is an effective method in quantifying the incremental improvements by adding some new predictors to the existing predictors.

Statistical analysis

To verify the balance between training and internal validation cohort, Mann-Whitney U tests were used for continuous clinical risk factors, Chi-squared tests were applied for categorical variables, and log-rank tests were conducted for DFS. A two-sided $P<0.05$ was deemed an attained statistical significance level. All tests were based on R packages (Supplemental Text S7) in R software (version 3.4.3; https://www.r-project.org/).

Results

Patient characteristics and radiomic feature discovery

Baseline characteristics of clinical risk factors for training, internal validation, and external validation cohorts are summarized in Table 1. Patients in the training and internal validation cohorts were balanced for survival with the median DFS of 25.5 months (observed: 58/166, 34.9%) and 22.0 months (observed: 33/83, 39.8%), respectively (P = 0.4290, log-rank test). No significant difference was captured between these two cohorts in clinical risk factors (P =

0.0656-0.9104). After univariate and multivariate Cox regression, only ctEMVI was identified as a significant prognostic factor (Table 2).

A total of 924 radiomic features were initially extracted per image, among which approximately 50% features were included in the subsequent experiments after data cleaning consistency test. LASSO Cox method identified four potential radiomic features (Supplemental Figure S3). Stratification ability and prognosis performance of each selected radiomic feature were revealed univariately in Supplemental Figure S4 and Table S2.

Radiomic signature construction and validation

With the regression coefficients of four selected radiomic features, formula for radiomic signature is defined in Supplemental Text S8. The radiomic signature alone was a risk factor for DFS in the training cohort (Table 2), and this was confirmed in both validation cohorts with the hazard ratio (HR) of 1.825 (95% confidence interval [CI]: 1.107-3.009) and 1.694 (95%CI: 1.220-2.352).

By the cutoff value 0.109 in the training cohort, patients in internal validation cohort were separated into high-risk group (range, 0.155-1.827) and low- risk group (range, -23.865-0.096). Radiomic signature of high-risk patients in external validation cohort were from 0.182 to 2.586, whereas low-risk values were from -20.374 to 0.039. The risk stratification ability of the radiomic signature was verified in both validation cohorts (P = 0.0260 and 0.0003, Figure 2). Normalized mean values of the four respective radiomic features for high-risk and low-risk patients are illustrated in a radar map (Supplemental Figure S5). The radiomic signature showed a fine distinguishing ability by a C-index of 0.695 (95%CI: 0.626-0.763) in the training cohort, 0.646 (95%CI: 0.560-0.731) in internal validation cohort, and 0.693 (95%CI: 0.617-0.770) in external validation cohort (Table 3).

Risk stratification ability of radiomic signature in subgroup analysis

The Kaplan-Meier survival curves with the previous cutoff value (0.109) are conducted within seven subgroups. In center 1, patients in ctT4, ctN+, and neoadjuvant therapy subgroups could be

significantly separated into high-risk and low-risk of DFS (P = 0.0019, 0.0058, 0.0008, Figure 3), while for ctT1, ctT2, ctT3, and ctN- patients, the radiomic signature may fail to well risk stratify them (Supplemental Figure S6) due to the nature of early clinical stage. In center 2, radiomic signature was again verified to work well with patients in ctT3, ctT4, ctN+, and neoadjuvant therapy subgroups (P = 0.0162, 0.0215, 0.0038, 0.0005, respectively).

Individualized Radiomic Nomogram

After univariate and multivariate Cox regression, ctEMVI and radiomic signature were identified as two significant prognostic factors. Considering the significance in univariate analysis and the great power in clinical prognosis prediction, we incorporated ctT and ctN in the radiomic nomogram. Thus, the radiomic nomogram combining the radiomic signature, ctEMVI, ctT, and ctN is presented in Figure 4a. Formula for radiomic nomogram is shown in Supplemental Text S8.

Calibration curves (Figure 4b) suggested good agreement between model predictions and actual outputs at 1, 2, and 3 years (Hosmer-Lemeshow test: P = 0.6849, 0.9177, 0.9571, respectively). Decision curves (Figure 4c) indicated that radiomic nomogram added more benefits when directing treatment strategies compared with radiomic signature, TNM staging model, and simple schemes (follow-up of all or none patients) across a threshold range of 0.00-0.64. Kaplan-Meier curves for radiomic nomogram are shown in Supplemental Figure S7.

In internal validation cohort, the predictive ability of radiomic nomogram (C-index [95%CI]: 0.720 [0.636-0.804]; AUCs of 0.696, 0.771, 0.708 at 1, 2, 3 years) outperformed the TNM staging model (C-index [95%CI]: 0.680 [0.548–0.812]; AUCs of 0.644, 0.677, 0.690 at 1, 2, 3 years). Time-dependent ROC curves are presented in Supplemental Figure S8. A significant difference was found in C-index between radiomic nomogram and radiomic signature (P = 0.0115), whereas there was no difference between radiomic nomogram and TNM staging model (P = 0.1981). In this case, however, an IDI of 16.6% (95%CI, 6.7%-34.6%; P<0.0001) did identify the promotion of radiomic nomogram compared with clinical prognosis by TNM staging

(Supplemental Figure S9). In external validation cohort, a C-index of 0.727 (95%CI: 0.662-0.792) from radiomic nomogram again surpassed 0.712 (95%CI: 0.614-0.810) from TNM staging model. Higher time-dependent AUCs (0.742, 0.765, 0.762 at 1, 2, 3 years) for radiomic nomogram were also achieved.

Discussion

The implementation of individualized strategies of gastric cancer may be promoted when radiomic approaches are adopted in preoperative prognostic models. To the best of our knowledge, few pioneering researches only concentrated on preoperative risk model construction for DFS in gastric cancer based on radiomics. In this study, we explored an MDCT-guided radiomic signature as an effective prognostic factor for preoperative risk stratification and verified the assistance of a radiomic nomogram to the prognosis prediction beyond ordinal staging system.

For a start, the significant differences of DFS between high-risk and low-risk groups separated by radiomic signature were demonstrated in both internal and external validation cohorts, as reported in previous studies on prognosis prediction by radiomics for gastric cancer and other cancers[18,23,24]. In order to further validate the risk stratification ability of radiomic signature in patients with certain clinical stage, subgroup analysis was performed. And similar results were obtained in both centers that significant differences of DFS between high-risk and low-risk groups occurred in relatively more advanced clinical stage (ctT3-4, ctN+, and neoadjuvant therapy groups), probably relevant to tumor heterogeneity and aggression. It shows the potentiality of radiomic signature in providing more evidence-based risk stratification instructions when treatment strategies need to be made. A gastric cancer patient with ctT4, for instance, advanced clinical stage is an evidence for accepting neoadjuvant therapy that may improve prognosis, and now belonging to high-risk group could be an additional proof.

Prognosis of gastric cancer lies in the interaction with patient-, tumor-, and treatment-related elements, however, the preoperative risk model can only be established on the first two. The

radiomic nomogram incorporated a radiomic signature revealing intratumor heterogeneity, a macroscopic finding on MDCT, and clinical staging information. This combined model reflected more comprehensive characteristics of gastric cancer and overcame the latent shortcoming of a single-sided model. The radiomic nomogram outperformed the conventional TNM staging model manifested by C-index, AUC, and DCA, indicating that radiomic approaches could aid preoperative prognosis estimation directly. Thereinto, though the radiomic signature showed lower C-index values than the TNM staging model, we conducted further statistical comparison and confirmed that there were no significant differences in C-index values between the two models in training and internal validation cohorts (student *t* test; $P = 0.1593$ and 0.3088). In other words, the radiomic signature had a similar distinguishing ability to the TNM staging model, echoing our original intention to combine the radiomic signature to improve clinical prognostic prediction, rather than replace the TNM staging system. Moreover, as a preoperative model, our radiomic nomogram achieved a similar predictive level to previous postoperative risk models of gastric cancer (without radiomic method)[25-28], and compared to the latter, it could serve as an effective noninvasive toolkit and provide substantial basis along with great timeliness for preoperative risk stratification, which may further benefit gastric cancer patients' initial individualized treatments.

There were three advantages of the proposed methods. First, we conducted sample size power analysis to ensure an appropriate study design (Supplemental Text S3). Though the overall sample size was not so big, the case size configurations for the three cohorts were all proper for model construction and validation, which was the basis of this radiomics study. As far as we know, seldom did previous radiomics studies report the sample size power analysis results. Second, we investigated the associations of radiomic features extracted from different MDCT image phases and proved that portal venous phase images might be more appropriate and stable for radiomic feature extraction in gastric cancer (Supplemental Text S9, Figure S10, Table S3, Table S4), which was partially consistent with previous studies[29-31]. Our results also showed that

most of the selected features from different MDCT image phases showed close correlations, and morphological features may be more stable for different MDCT image phases. Third, clearer than previous studies, we specified ICC calculation models, making consistency tests by ICC more reasonable. Moreover, comparative experiments using different feature selection methods were conducted (Supplemental Text S10, Table S5, Table S6), proving that the presented methods were competitive. Also, the proposed methods along with radiomic signature performance were equivalent to previous studies (C-index = 0.695-0.700)[17,18].

The four MDCT-derived radiomic features were consistent with previous biomarker findings for gastric cancer or survival[32-34]. Given the radiomics hypothesis, greater major axis length and median intensity values demonstrate larger tumor size, probably in accord with higher disease occurrence probability and poorer prognosis. Lower small zone emphasis values and greater zone size non-uniformity values are possibly indicative of more intratumor heterogeneity and worse survival. The interpretations above are in concordance with radiomic signature formula. For another, although not all the radiomic features stratified patients univariately or achieved fine single C-index, the multi-feature radiomic signature and the combined radiomic nomogram did predict survival outcomes well, similar to the common sense that doctors naturally correlate multiple estimations of disease as opposed to focusing on a single factor to determine therapy in clinical practice[35].

For all cancers, the direct relationship between TNM classification and prognosis is a well-established basis for treatment. In univariate analysis, there were significant associations between ctT/ctN and DFS, indicating great power of the two factors in prognosis. Therefore, we incorporated ctT and ctN in the radiomic nomogram. However, ctT and ctN were not significantly associated with DFS in multivariate analysis. This could be induced by inaccurate preoperative clinical staging. The accuracies of T/N stage defined on MDCT were just 62-75% and 75-80% with postoperative pathological staging as the gold standard[2,36,37]. Another reason may be the small sample size of this retrospective study, thus failing to detect important clinical

findings sufficiently[38]. However, considering the clinical significance of ctT and ctN, the two factors also participated in the radiomic nomogram construction, the results of which showed better predictive ability, surpassing the radiomic signature and conventional TNM staging model.

As for EMVI, the presence of malignant cells within blood vessels beyond the muscularis propria, was confirmed closely related to poor outcomes of patients with gastrointestinal tumors[6,39,40] and used to develop magnetic resonance imaging (MRI)-based risk stratification models[41,42]. However, MRI has great limitation in diagnosing EMVI accurately due to motion artifacts[43]. In this study, ctEMVI was identified as an significant predictor, which agreed with several studies[5,6,44] that had discovered ctEMVI as an independent risk factor for the prognosis of gastric cancer.

This study also has some limitations. First, the sample size for this multicenter retrospective study was still not enough and a relatively short follow-up period may result in bias. Second, tumor delineation was not automatically performed, making it a time-consuming and labor-intensive task. Third, the differences of DFS between the two centers may account for the time-dependent AUCs in external validation cohort being slightly higher than those in the training cohort, which may be caused by different follow-up strategies in different centers. Finally, accurate pathological diagnosis of EMVI is based on pathological large section technique which can show the tumors and surrounding tissues in an overall and comprehensive way. But pathological large section examination for gastric cancer is not routinely used in clinical work in most hospitals, including the centers in our research, therefore, ctEMVI cannot be confirmed by pathology universally. However, we believe our study showed the potential of using radiomics in daily practice and offering help in individualized strategies.

Conclusions

The radiomic signature established in this study was a validated independent prognostic factor in gastric cancer. The radiomic nomogram improved the predictive performance of preoperative staging model, probably providing a new train of thought beyond clinical prognosis and risk

stratification in individualized treatment strategies for gastric cancer.

Acknowledgments

We appreciate Haidong Xiang and Xiaoxuan Jia for their help in gathering data for this study. This work was supported by the National Key R&D Program of China (2017YFC1308700, 2017YFA0205200, 2017YFC1309100), National Natural Science Foundation of China (81901819, 91959130, 81971776, 81771924, 81930053, 81227901, 81671851, 81527805, 81771912), the Beijing Natural Science Foundation (L182061), the Bureau of International Cooperation of Chinese Academy of Sciences (173211KYSB20160053), Strategic Priority CAS Project (XDB38040200), and the Youth Innovation Promotion Association CAS (2017175).

Conflict of Interest Statement

The authors have no relevant conflicts of interest to disclose.

Data Sharing and Data Accessibility

The datasets used and analyzed during the current study are available from the corresponding author on reasonable request.

Figure Legends

Figure 1. The overall radiomics workflow. (a) Examples of manual tumor delineation on multidetector-row computed tomography. (b) Feature discovery, including radiomic feature selection and clinical characteristic analysis. (c) Radiomic signature and radiomic nomogram construction. (d) Model performance evaluation. ICC, intraclass correlation coefficient; LASSO, least absolute shrinkage selection operator; KM, Kaplan-Meier; AUC, area under the curve; DCA, decision analysis curve; IDI, integrated discrimination improvement.

Figure 2. Kaplan-Meier survival curves indicated the radiomic signature could risk stratify gastric cancer patients in the (a) training cohort, (b) internal validation cohort, and (c) external validation cohort.

Figure 3. Subgroup analysis showed that radiomic signature had good risk-stratification ability

for patients with more advanced clinical stage. Center 1: (a) ctT4 subgroup, (b) ctN+ subgroup, (c) neoadjuvant therapy subgroup. Center 2: (d) ctT4 subgroup, (e) ctN+ subgroup, (f) neoadjuvant therapy subgroup. ctT, clinical T stage defined on multidetector-row computed tomography; ctN, clinical N stage defined on multidetector-row computed tomography.

Figure 4. (a) A radiomic nomogram combined ctT, ctN, ctEMVI, and radiomic signature. (b) Calibration curves. (c) Decision curve analysis for radiomic nomogram (red line), follow-up of all (blue line), follow-up of none (black line), radiomic signature (orange line), and TNM staging model (green line) in internal validation cohort. ctT, clinical T stage defined on MDCT; ctN, clinical N stage defined on MDCT; ctEMVI, extramural vessel invasion defined on MDCT; MDCT, multidetector-row computed tomography; DFS, disease-free survival; TNM, tumor-node-metastasis.

References

1. Bray F, Ferlay J, Soerjomataram I, Siegel RL, Torre LA, Jemal A. Global cancer statistics 2018: GLOBOCAN estimates of incidence and mortality worldwide for 36 cancers in 185 countries. *CA: a cancer journal for clinicians.* 2018;68(6):394-424.

2. Saito T, Kurokawa Y, Takiguchi S, et al. Accuracy of multidetector-row CT in diagnosing lymph node metastasis in patients with gastric cancer. *European radiology.* 2015;25(2):368-374.

3. Bando E, Makuuchi R, Irino T, Tanizawa Y, Kawamura T, Terashima M. Validation of the prognostic impact of the new tumor-node-metastasis clinical staging in patients with gastric cancer. *Gastric Cancer.* 2019:1-7.

4. Li J-H, Shen W-Z, Gu X-Q, Hong W-K, Wang Z-Q. Prognostic value of EUS combined with MSCT in predicting the recurrence and metastasis of patients with gastric cancer. *Japanese journal of clinical oncology.* 2017;47(6):487-493.

5. Cheng J, Feng C, Zhang Y, Hong N, Ye Y, Wang Y. CT-Detected Extramural Vessel Invasion and Regional Lymph Node Involvement in Stage T4a Gastric Cancer for Predicting Progression-Free Survival. *American Journal of Roentgenology.* 2019:1-7.

6. Kim TU, Kim S, Lee NK, et al. Prognostic Value of Computed Tomography–Detected Extramural Venous Invasion to Predict Disease-Free Survival in Patients With Gastric Cancer. *Journal of computer assisted tomography.* 2017;41(3):430-436.

7. Wang K, Liang Q, Li X, et al. MDGA2 is a novel tumour suppressor cooperating with DMAP1 in gastric cancer and is associated with disease outcome. *Gut.* 2016;65(10):1619-1631.

8. Chan THM, Qamra A, Tan KT, et al. ADAR-mediated RNA editing predicts progression and prognosis of gastric cancer. *Gastroenterology.* 2016;151(4):637-650. e610.

9. Zhang B, Tian J, Dong D, et al. Radiomics features of multiparametric MRI as novel prognostic factors in advanced nasopharyngeal carcinoma. *Clinical Cancer Research.* 2017;23(15):4259-4269.

10. Meng Y, Zhang Y, Dong D, et al. Novel radiomic signature as a prognostic biomarker for locally advanced rectal cancer. *Journal of Magnetic Resonance Imaging.* 2018;48(3):605-614.

11. Dong D, Tang L, Li Z-Y, et al. Development and validation of an individualized nomogram to identify occult peritoneal metastasis in patients with advanced gastric cancer. *Annals of Oncology.* 2019.

12. Aerts HJWL, Velazquez ER, Leijenaar RTH, et al. Decoding tumour phenotype by noninvasive imaging using a quantitative radiomics approach. *Nature Communications.* 2014;5:4006.

13. Lambin P, Leijenaar RTH, Deist TM, et al. Radiomics: the bridge between medical

imaging and personalized medicine. *Nature Reviews Clinical Oncology.* 2017;14(12):749-762.

14. Giganti F, Antunes S, Salerno A, et al. Gastric cancer: texture analysis from multidetector computed tomography as a potential preoperative prognostic biomarker. *European radiology.* 2017;27(5):1831-1839.

15. Yoon SH, Kim YH, Lee YJ, et al. Tumor heterogeneity in human epidermal growth factor receptor 2 (HER2)-positive advanced gastric cancer assessed by CT texture analysis: association with survival after trastuzumab treatment. *PloS one.* 2016;11(8):e0161278.

16. Li W, Zhang L, Tian C, et al. Prognostic value of computed tomography radiomics features in patients with gastric cancer following curative resection. *European radiology.* 2019;29(6):3079-3089.

17. Jiang Y, Chen C, Xie J, et al. Radiomics signature of computed tomography imaging for prediction of survival and chemotherapeutic benefits in gastric cancer. *EBioMedicine.* 2018;36:171-182.

18. Jiang Y, Yuan Q, Lv W, et al. Radiomic signature of 18F fluorodeoxyglucose PET/CT for prediction of gastric cancer survival and chemotherapeutic benefits. *Theranostics.* 2018;8(21):5915.

19. Bradburn MJ, Clark TG, Love SB, Altman DG. Survival analysis part II: multivariate data analysis–an introduction to concepts and methods. *British journal of cancer.* 2003;89(3):431-436.

20. Kamarudin AN, Cox T, Kolamunnage-Dona R. Time-dependent ROC curve analysis in medical research: current methods and applications. *BMC medical research methodology.* 2017;17(1):53.

21. Bollschweiler E, Boettcher K, Hoelscher AH, et al. Is the prognosis for Japanese and

German patients with gastric cancer really different? *Cancer.* 1993;71(10):2918-2925.

22. Uno H, Tian L, Cai T, Kohane IS, Wei L. A unified inference procedure for a class of measures to assess improvement in risk prediction systems with survival data. *Statistics in medicine.* 2013;32(14):2430-2442.

23. Huang Y, Liu Z, He L, et al. Radiomics signature: a potential biomarker for the prediction of disease-free survival in early-stage (I or II) non-small cell lung cancer. *Radiology.* 2016;281(3):947-957.

24. Park H, Lim Y, Ko ES, et al. Radiomics signature on magnetic resonance imaging: association with disease-free survival in patients with invasive breast cancer. *Clinical Cancer Research.* 2018;24(19):4705-4714.

25. Han D-S, Suh Y-S, Kong S-H, et al. Nomogram predicting long-term survival after d2 gastrectomy for gastric cancer. *J Clin Oncol.* 2012;30(31):3834-3840.

26. Kattan MW, Karpeh MS, Mazumdar M, Brennan MF. Postoperative nomogram for disease-specific survival after an R0 resection for gastric carcinoma. *Journal of clinical oncology.* 2003;21(19):3647-3650.

27. Hirabayashi S, Kosugi S, Isobe Y, et al. Development and external validation of a nomogram for overall survival after curative resection in serosa-negative, locally advanced gastric cancer. *Annals of oncology.* 2014;25(6):1179-1184.

28. Kim Y, Spolverato G, Ejaz A, et al. A nomogram to predict overall survival and disease-free survival after curative resection of gastric adenocarcinoma. *Annals of surgical oncology.* 2015;22(6):1828-1835.

29. Meng X, Ni C, Shen Y, et al. Differentiating malignant from benign gastric mucosal lesions with quantitative analysis in dual energy spectral computed tomography: Initial experience. *Medicine.* 2017;96(2).

30. Li R, Li J, Wang X, Liang P, Gao J. Detection of gastric cancer and its histological type based on iodine concentration in spectral CT. *Cancer Imaging.* 2018;18(1):1-10.

31. Liu S, Shi H, Ji C, et al. Preoperative CT texture analysis of gastric cancer: correlations with postoperative TNM staging. *Clinical radiology.* 2018;73(8):756. e751-756. e759.

32. Hou Z, Yang Y, Li S, et al. Radiomic analysis using contrast-enhanced CT: predict treatment response to pulsed low dose rate radiotherapy in gastric carcinoma with abdominal cavity metastasis. *Quantitative imaging in medicine and surgery.* 2018;8(4):410.

33. Zhai T-T, van Dijk LV, Huang B-T, et al. Improving the prediction of overall survival for head and neck cancer patients using image biomarkers in combination with clinical parameters. *Radiotherapy and Oncology.* 2017;124(2):256-262.

34. Zhou H, Dong D, Chen B, et al. Diagnosis of distant metastasis of lung cancer: Based on clinical and radiomic features. *Translational oncology.* 2018;11(1):31-36.

35. Moons KG, Altman DG, Reitsma JB, et al. Transparent Reporting of a multivariable prediction model for Individual Prognosis or Diagnosis (TRIPOD): explanation and elaboration. *Annals of internal medicine.* 2015;162(1):W1-W73.

36. Yan C, Zhu ZG, Yan M, et al. Value of multidetector‐row computed tomography in the preoperative T and N staging of gastric carcinoma: A large‐scale Chinese study. *Journal of surgical oncology.* 2009;100(3):205-214.

37. Joo I, Lee JM, Kim JH, Shin CI, Han JK, Choi BI. Prospective comparison of 3T MRI with diffusion‐weighted imaging and MDCT for the preoperative TNM staging of gastric cancer. *Journal of Magnetic Resonance Imaging.* 2015;41(3):814-821.

38. Iasonos A, Schrag D, Raj GV, Panageas KS. How to build and interpret a nomogram for cancer prognosis. *Journal of clinical oncology.* 2008;26(8):1364-1370.

39. Gibson KM, Chan C, Chapuis PH, Dent OF, Bokey L. Mural and extramural venous invasion and prognosis in colorectal cancer. *Diseases of the colon & rectum.* 2014;57(8):916-926.

40. Yao X, Yang S-X, Song X-H, Cui Y-C, Ye Y-J, Wang Y. Prognostic significance of computed tomography-detected extramural vascular invasion in colon cancer. *World journal of gastroenterology.* 2016;22(31):7157.

41. Battersby NJ, How P, Moran B, et al. Prospective validation of a low rectal cancer magnetic resonance imaging staging system and development of a local recurrence risk stratification model. *Annals of surgery.* 2016;263(4):751-760.

42. Siddiqui MR, Simillis C, Hunter C, et al. A meta-analysis comparing the risk of metastases in patients with rectal cancer and MRI-detected extramural vascular invasion (mrEMVI) vs mrEMVI-negative cases. *British journal of cancer.* 2017;116(12):1513-1519.

43. Giganti F, Orsenigo E, Arcidiacono PG, et al. Preoperative locoregional staging of gastric cancer: is there a place for magnetic resonance imaging? Prospective comparison with EUS and multidetector computed tomography. *Gastric Cancer.* 2016;19(1):216-225.

44. Cheng J, Wu J, Ye Y, Zhang C, Zhang Y, Wang Y. The prognostic significance of extramural venous invasion detected by multiple-row detector computed tomography in stage III gastric cancer. *Abdominal radiology.* 2016;41(7):1219-1226.

Table 1. Baseline characteristics of clinical risk factors for enrolled gastric cancer patients.

Clinical risk factors	Training cohort (n=166)	Internal validation cohort (n=83)	*P*	External validation cohort (n=104)
Age, mean ± SD, years	64.1±12.3	61.3±12.9	0.1061	57.5±11.2
Sex, No. (%)			0.8398	
male	122 (73.5)	60 (72.3)		72 (69.2)
female	44 (26.5)	23 (27.7)		32 (30.8)
CEA, median (IQR)	2.00 (1.17-3.39)	1.57 (0.92-2.70)	0.0656	2.00 (1.00-4.00)
CA19-9, median (IQR)	11.66 (7.86-22.88)	10.74 (5.84-22.80)	0.5287	11.00 (7.00-20.00)
Location/growth pattern, No. (%)			0.7011	
Distal nondiffusion	114 (68.7)	55 (66.3)		96 (92.3)
Diffusion/proximal nondiffusion	52 (31.3)	28 (33.7)		8 (7.7)
ctT, No. (%)			0.9104	
T1-2	17 (10.2)	10 (12.0)		22 (21.2)
T3	37 (22.3)	18 (21.7)		35 (33.7)
T4	112 (67.5)	55 (66.3)		47 (45.1)
ctN, No. (%)			0.7868	
N-	91 (54.8)	47 (56.6)		43 (41.3)
N+	75 (45.2)	36 (43.4)		61 (58.7)
ctEMVI, No. (%)			0.7836	
Negative	99 (59.6)	51 (61.4)		60 (57.7)
Positive	67 (40.4)	32 (38.6)		44 (42.3)

Survival outcomes		0.4290	
DFS time, median (IQR), months	25.5 (12.0-46.0)	22.0 (12.0-45.0)	58.0 (33.0-71.5)
DFS event, No. (%)			
Disease progression	58 (34.9)	33 (39.8)	40 (38.5)
No disease progression	108 (65.1)	50 (60.2)	64 (61.5)

NOTE. *P* values were calculated to verify the balance between the training and internal validation cohorts. Mann-Whitney U tests were used for continuous clinical risk factors, Chi-squared tests were applied for categorical variables, and log-rank test was conducted for survival outcomes. CEA, carcinoembryonic antigen, CA19-9, carbohydrate antigen 19-9; ctT, clinical T stage defined on MDCT; ctN, clinical N stage defined on MDCT; ctEMVI, extramural vessel invasion defined on MDCT; MDCT, multidetector-row computed tomography; DFS, disease-free survival; SD, standard deviation; IQR, interquartile range.

Table 2. Univariate and multivariate Cox regression analysis for clinical risk factors and radiomic signature in the training cohort.

Factors	Univariate Cox regression		Multivariate Cox regression	
	HR (95% CI)	*P* value	HR (95% CI)	*P* value
Age	1.009 (0.987-1.032)	0.4085	1.076 (0.723-1.601)	0.7176
Sex				
Male	1 (reference)		1 (reference)	
Female	0.710 (0.382-1.319)	0.2784	0.691 (0.359-1.328)	0.2670
CEA	1.004 (1.001-1.008)	**0.0054**	1.003 (0.995-1.011)	0.4620
CA19-9	1.001 (1.000-1.002)	**0.0154**	0.996 (0.977-1.016)	0.6915
Location/growth pattern				
Distal nondiffusion	1 (reference)		1 (reference)	
Diffusion/proximal nondiffusion	3.005 (1.789-5.048)	**<0.0001**	1.411 (0.722-2.760)	0.3140
ctT				
T1-2	1 (reference)		1 (reference)	
T3	3.030 (0.365-25.157)	0.3047	1.622 (0.185-14.200)	0.6624
T4	9.889 (1.367-71.569)	**0.0233**	1.946 (0.234-16.175)	0.5379
ctN				
N−	1 (reference)		1 (reference)	
N+	2.583 (1.509-4.421)	**0.0005**	1.246 (0.680-2.282)	0.4774
ctEMVI				

Negative	1 (reference)		1 (reference)	
Positive	5.377 (2.982-9.696)	**<0.0001**	2.671 (1.266-5.634)	**0.0099**
Radiomic signature	2.718 (1.965-3.761)	**<0.0001**	1.543 (1.106-2.155)	**0.0108**

NOTE. *P* values were calculated via Wald tests and bold values represented $P < 0.05$. HR, hazard ratio; CI, confidence interval; CEA, carcinoembryonic antigen; CA19-9, carbohydrate antigen 19-9; ctT, clinical T stage defined on MDCT; ctN, clinical N stage defined on MDCT; ctEMVI, extramural vessel invasion defined on MDCT; MDCT, multidetector-row computed tomography.

Table 3. Performance of prognostic models.

Cohorts	Prognostic models	Parameters						
		C-index (95% CI)	HR		Time-dependent AUC			AIC
			HR (95% CI)	*P* value	1-year	2-year	3-year	
Training								
	Radiomic nomogram	0.760 (0.696-0.824)	2.743 (2.054-3.665)	<0.0001	0.725	0.765	0.786	497.22
	Radiomic signature	0.694 (0.626-0.763)	2.718 (1.965-3.761)	<0.0001	0.650	0.658	0.711	512.07
	TNM staging model	0.742 (0.648-0.837)	2.728 (1.687-4.411)	<0.0001	0.667	0.688	0.692	523.27
Internal validation								
	Radiomic nomogram	0.720 (0.636-0.804)	2.411 (1.565-3.715)	0.0091	0.696	0.771	0.708	
	Radiomic signature	0.646 (0.560-0.731)	1.825 (1.107-3.009)	0.1169	0.665	0.695	0.587	
	TNM staging model	0.680 (0.548-0.812)	1.924 (1.129-3.281)	0.0134	0.644	0.677	0.690	
External validation								
	Radiomic nomogram	0.727 (0.662-0.792)	2.060 (1.482-2.863)	0.0014	0.742	0.765	0.762	
	Radiomic signature	0.693 (0.617-0.770)	1.694 (1.220-2.352)	0.0243	0.656	0.689	0.706	

TNM staging model	0.712 (0.614-0.810)	1.913 (1.274-2.873)	0.0012	0.712	0.688	0.709

NOTE. Lower AIC values represented more generalized models. C-index, concordance index; CI, confidence interval; HR, hazard ratio; AUC, area under the curve; AIC, Akaike information criterion; TNM, tumor-node-metastasis.

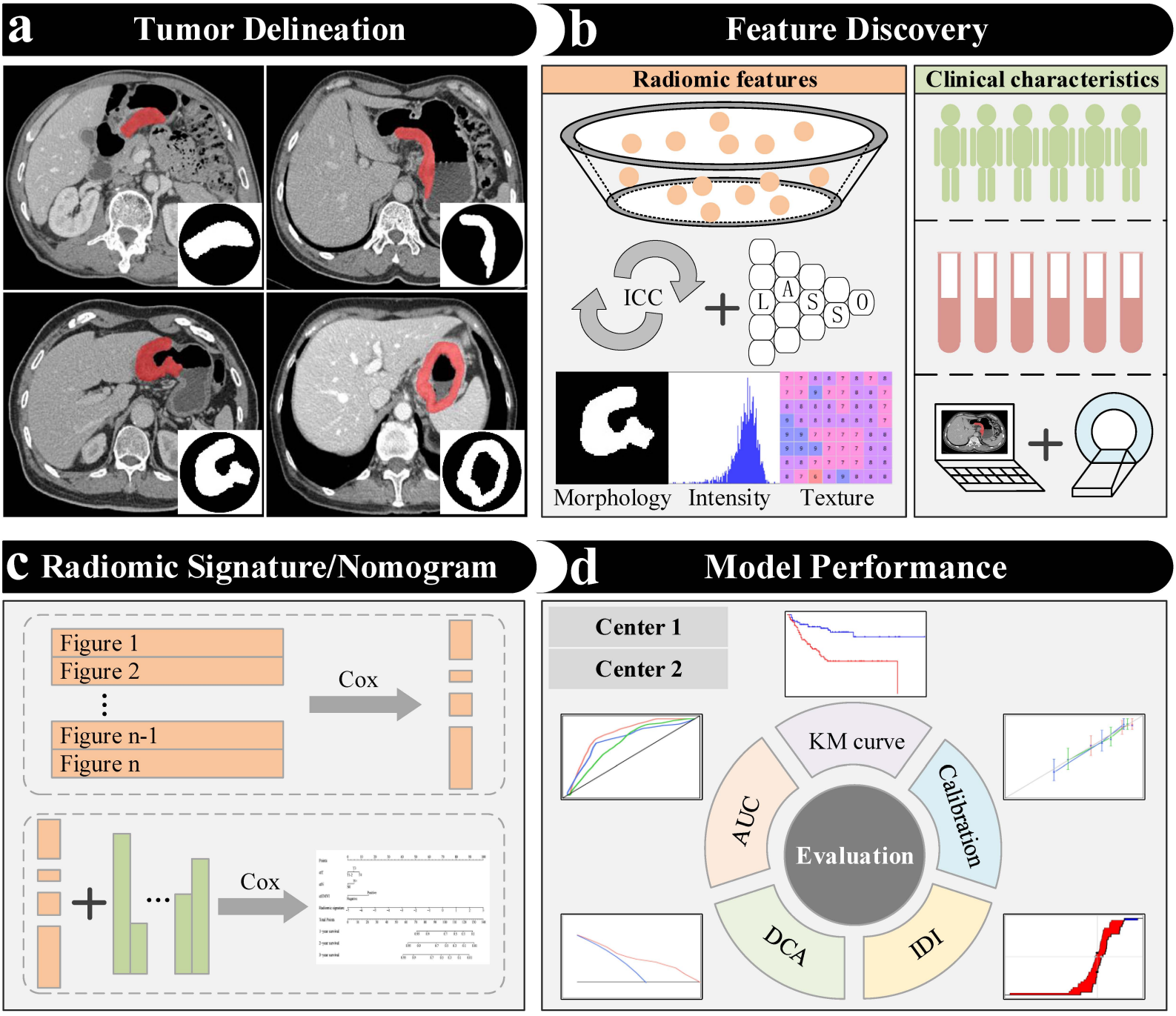
a
Tumor Delineation
b
Feature Discovery
Radiomic features
Clinical characteristics
ICC
L A S S O
Morphology
Intensity
Texture
c
Radiomic Signature/Nomogram
Figure 1
Figure 2
Figure n-1
Figure n
Cox
Cox
d
Model Performance
Center 1
Center 2
KM curve
Calibration
IDI
DCA
AUC
Evaluation

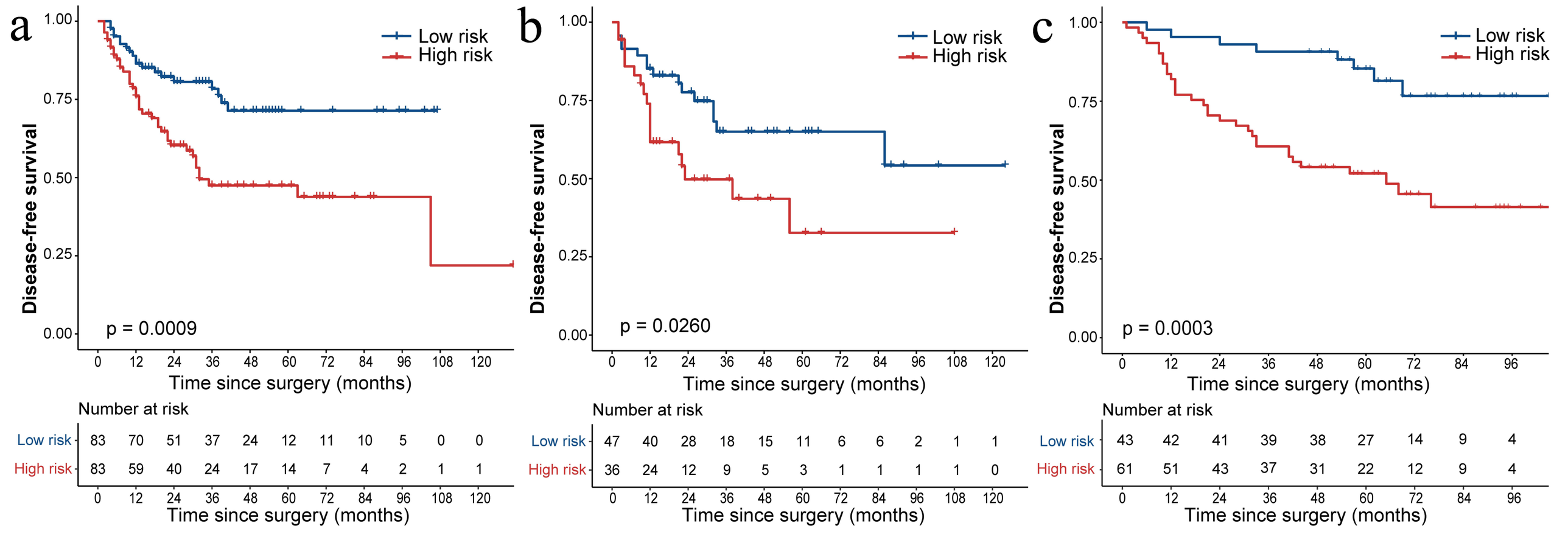
a
b
c
Low risk
High risk
Disease-free survival
1.00
0.75
0.50
0.25
0.00
p = 0.0009
p = 0.0260
p = 0.0003
0 12 24 36 48 60 72 84 96 108 120
Time since surgery (months)
Number at risk
Low risk 83 70 51 37 24 12 11 10 5 0 0
High risk 83 59 40 24 17 14 7 4 2 1 1
Low risk 47 40 28 18 15 11 6 6 2 1 1
High risk 36 24 12 9 5 3 1 1 1 1 0
Low risk 43 42 41 39 38 27 14 9 4
High risk 61 51 43 37 31 22 12 9 4

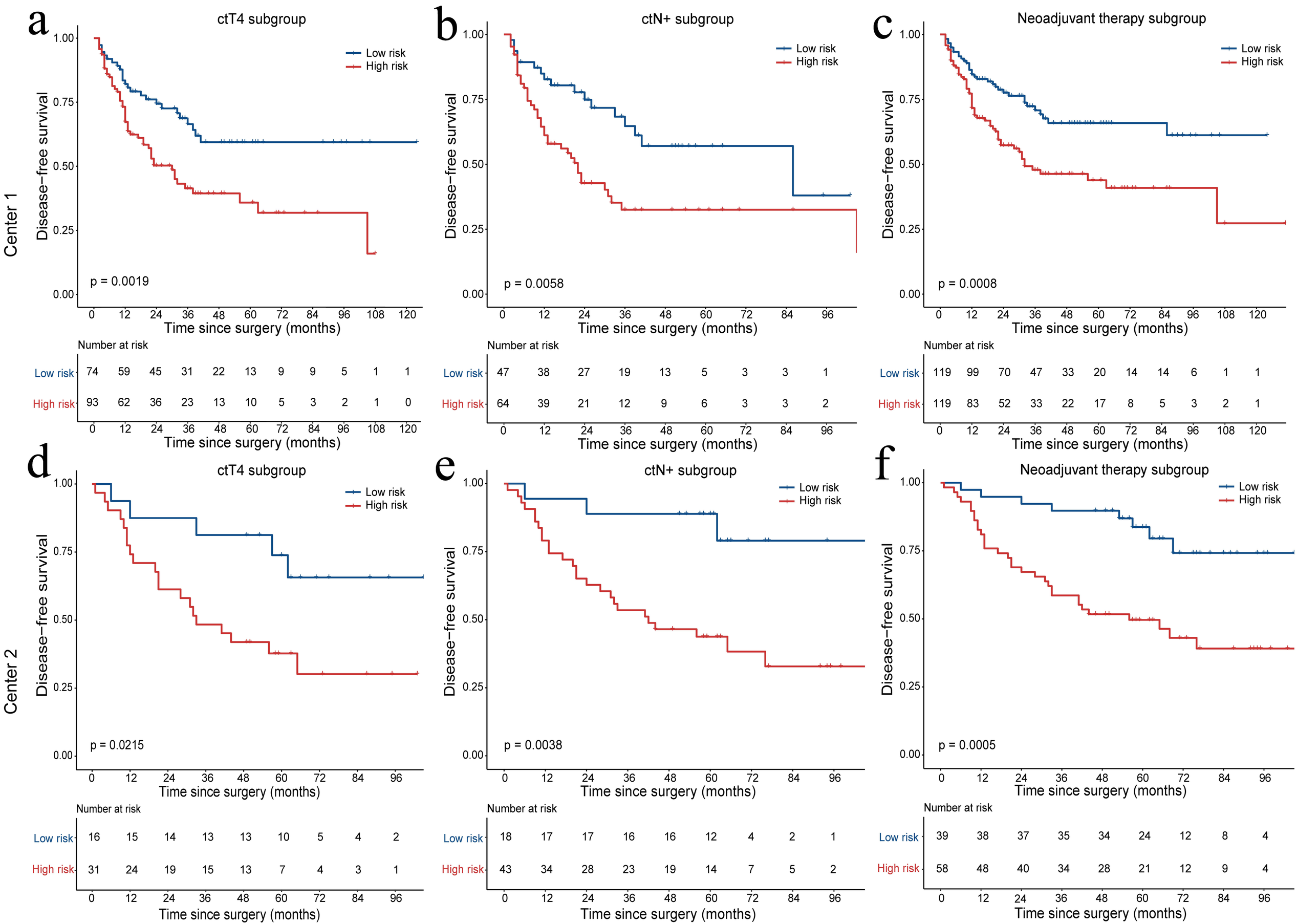
a
ctT4 subgroup
Low risk
High risk
Disease−free survival
p = 0.0019
Time since surgery (months)
Number at risk
Low risk 74 59 45 31 22 13 9 9 5 1 1
High risk 93 62 36 23 13 10 5 3 2 1 0
0 12 24 36 48 60 72 84 96 108 120
b
ctN+ subgroup
p = 0.0058
Number at risk
Low risk 47 38 27 19 13 5 3 3 1
High risk 64 39 21 12 9 6 3 3 2
0 12 24 36 48 60 72 84 96
c
Neoadjuvant therapy subgroup
p = 0.0008
Number at risk
Low risk 119 99 70 47 33 20 14 14 6 1 1
High risk 119 83 52 33 22 17 8 5 3 2 1
0 12 24 36 48 60 72 84 96 108 120
Center 1
d
ctT4 subgroup
p = 0.0215
Number at risk
Low risk 16 15 14 13 13 10 5 4 2
High risk 31 24 19 15 13 7 4 3 1
0 12 24 36 48 60 72 84 96
e
ctN+ subgroup
p = 0.0038
Number at risk
Low risk 18 17 17 16 16 12 4 2 1
High risk 43 34 28 23 19 14 7 5 2
0 12 24 36 48 60 72 84 96
f
Neoadjuvant therapy subgroup
p = 0.0005
Number at risk
Low risk 39 38 37 35 34 24 12 8 4
High risk 58 48 40 34 28 21 12 9 4
0 12 24 36 48 60 72 84 96
Center 2

a

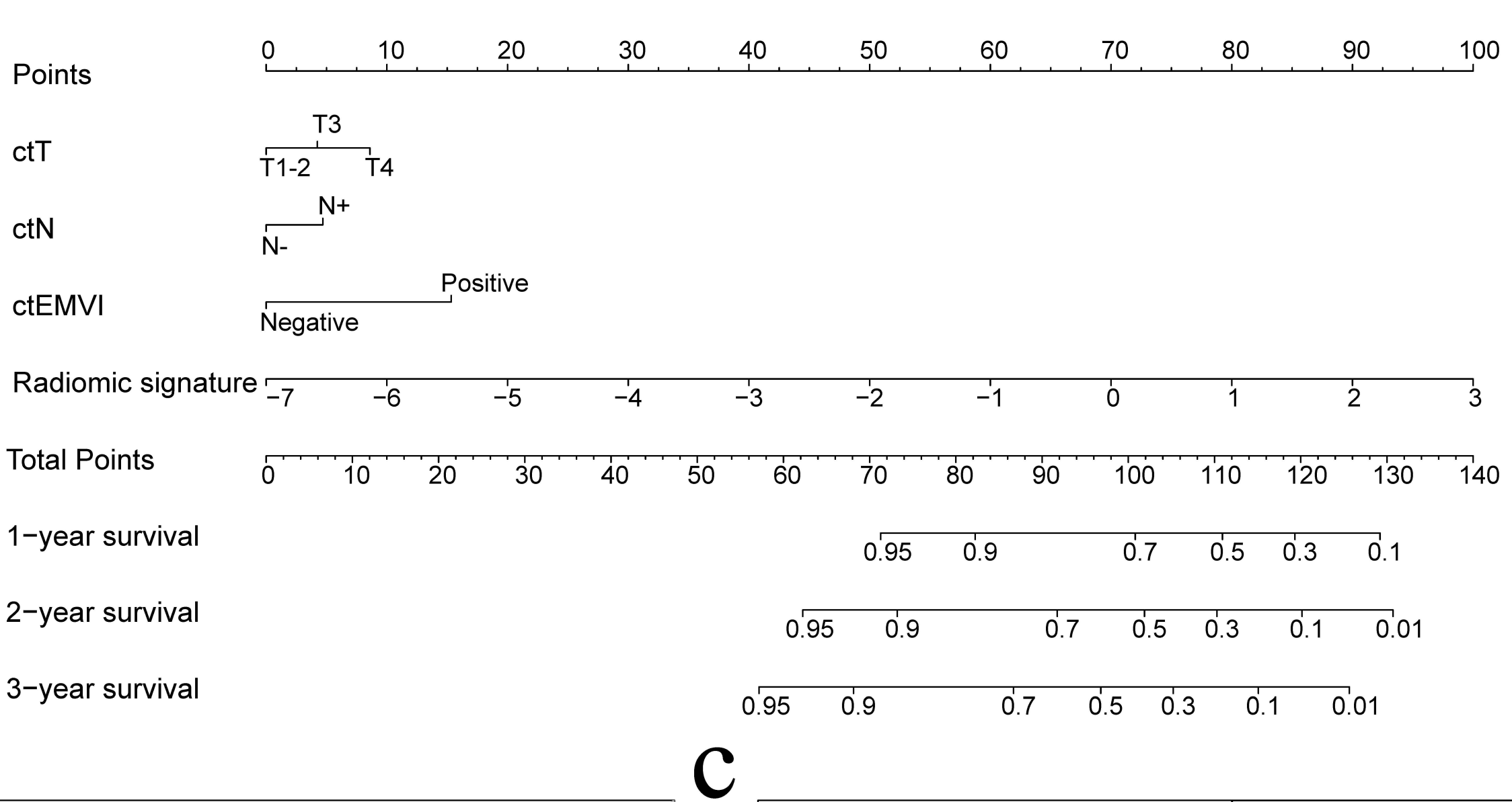
Points
0 10 20 30 40 50 60 70 80 90 100
ctT
T3
T1-2
T4
ctN
N+
N-
ctEMVI
Positive
Negative
Radiomic signature
−7 −6 −5 −4 −3 −2 −1 0 1 2 3
Total Points
0 10 20 30 40 50 60 70 80 90 100 110 120 130 140
1−year survival
0.95 0.9 0.7 0.5 0.3 0.1
2−year survival
0.95 0.9 0.7 0.5 0.3 0.1 0.01
3−year survival
0.95 0.9 0.7 0.5 0.3 0.1 0.01

b

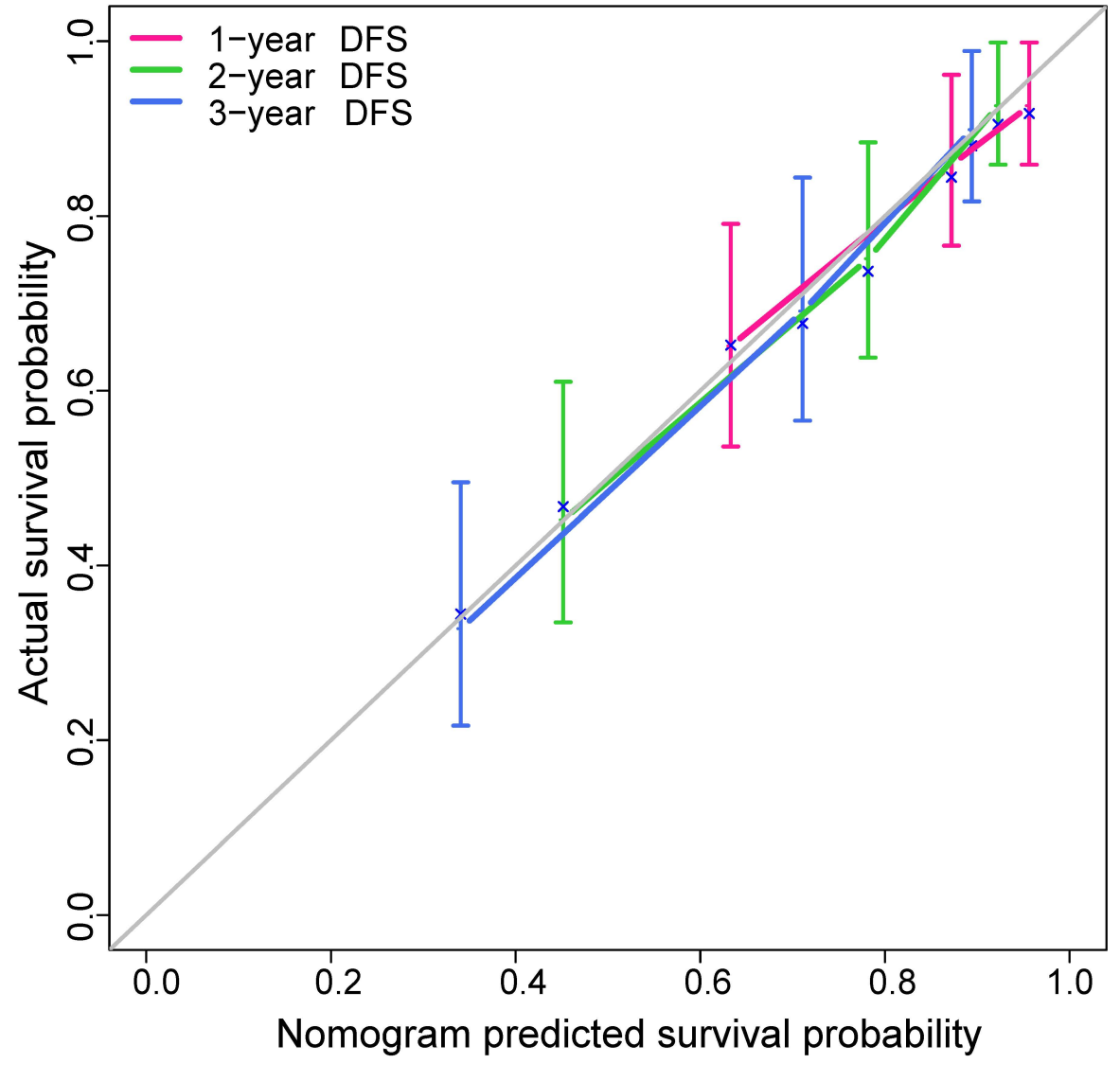
1−year DFS
2−year DFS
3−year DFS
Actual survival probability
0.0 0.2 0.4 0.6 0.8 1.0
Nomogram predicted survival probability
0.0 0.2 0.4 0.6 0.8 1.0

c

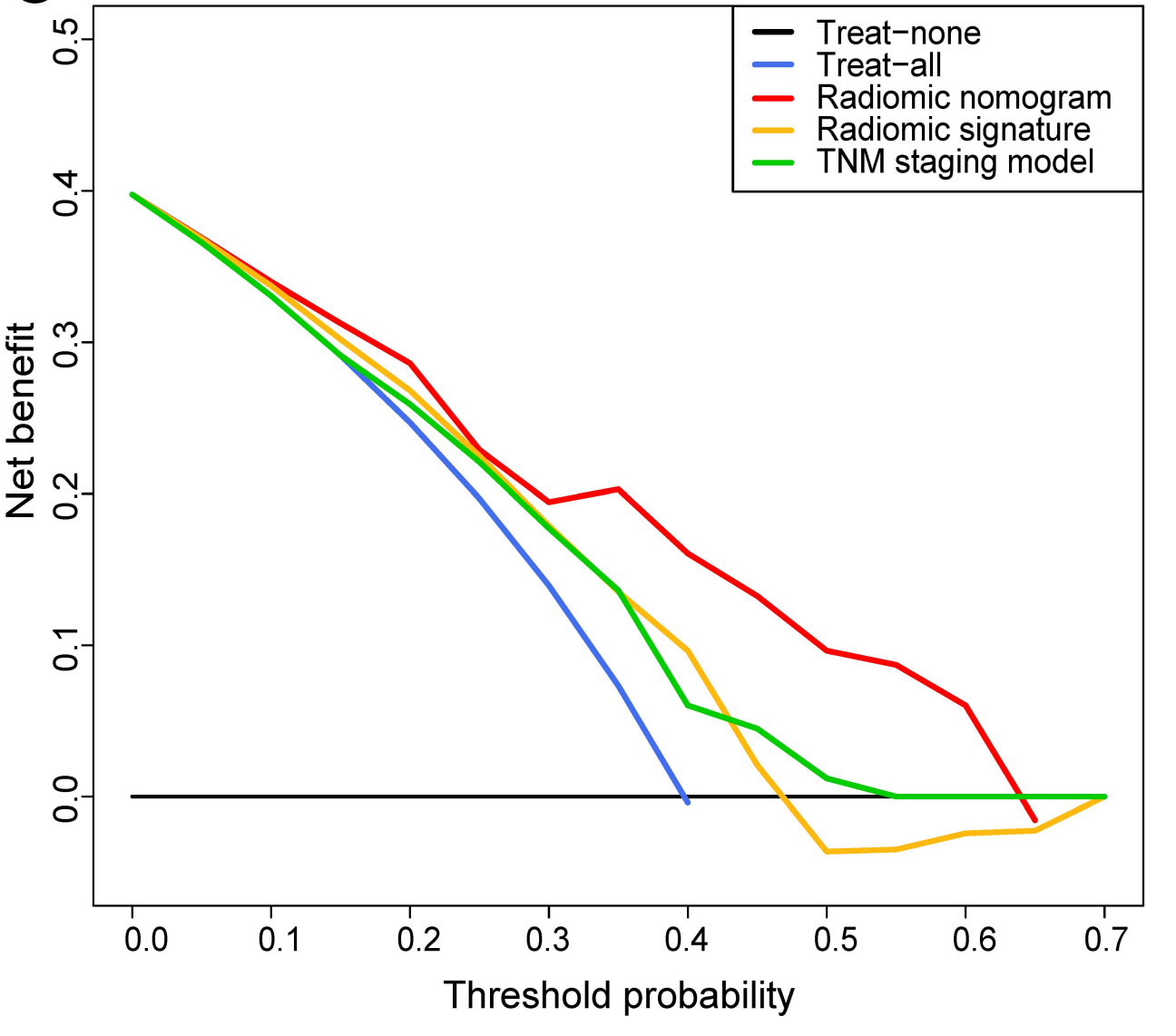
Treat−none
Treat−all
Radiomic nomogram
Radiomic signature
TNM staging model
Net benefit
0.0 0.1 0.2 0.3 0.4 0.5
Threshold probability
0.0 0.1 0.2 0.3 0.4 0.5 0.6 0.7